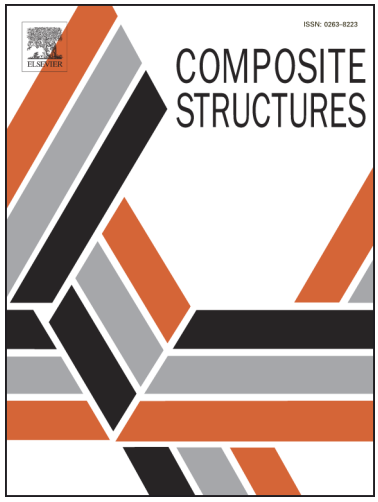

The Static and Dynamic Response of CFRP Tube Reinforced Polyurethane

A. Jamil, Z.W. Guan, W.J. Cantwell

PII: S0263-8223(16)32403-5
DOI: http://dx.doi.org/10.1016/j.compstruct.2016.11.043
Reference: COST 8003

To appear in: *Composite Structures*

Please cite this article as: Jamil, A., Guan, Z.W., Cantwell, W.J., The Static and Dynamic Response of CFRP Tube Reinforced Polyurethane, *Composite Structures* (2016), doi: http://dx.doi.org/10.1016/j.compstruct.2016.11.043

The Static and Dynamic Response of CFRP Tube Reinforced Polyurethane

A. Jamil[a,*], Z. W. Guan[a,b], W. J. Cantwell[c]

[a] *School of Engineering, University of Liverpool, Liverpool L69 3GH, UK*
[b] *School of Mechanical Engineering, Chengdu University, Shiling Town, Chengdu City, Sichuan Province, P.R.C.*
[c] *Department of Aerospace Engineering, Khalifa University of Science, Technology and Research (KUSTAR), Abu Dhabi, United Arab Emirates*

Abstract

This paper presents an investigation on the mechanical properties of thermosetting polyurethane (TSPU) and thermoplastic polyurethane (TPU) under quasi-static and low velocity impact (LVI) loading. Hollow glass microspheres were added at different volume percentages to the TSPU to decrease the density and to investigate the effect on the mechanical properties. Incorporating the fillers leads to the development of a stepwise graded foam, which has been shown to yield more constant plateau stress levels under dynamic loading. The work was extended to investigate reinforcing the TSPU and the TPU matrix with carbon fibre reinforced plastic (CFRP) tubes, providing a higher load-bearing capacity under static loading. Reinforcing the syntactic TSPU resulted in a 47.7 % increase in specific energy absorption (SEA), with the average value reaching 56.28 kJ/kg. The specific compressive strength for the reinforced TSPU was also improved under quasi-static loading, where a 65 % increase was observed, relative to the unreinforced TSPU. For the reinforced TPU significant improvements were seen under dynamic loading conditions, relative to the unreinforced TPU, with increases in plateau stress levels of 629 % and 452 % at strain levels of 25 % and 50 %, respectively.

Keywords:
carbon fibre, dynamic, energy absorption, mechanical testing, polyurethane, reinforcement, thermoset, thermoplastic

*Corresponding author
Email address: ajamil@liverpool.ac.uk (A. Jamil)

1. Introduction

Polyurethane is a versatile and widely used polymer that is available in the form of either thermoplastic polyurethane (TPU) or thermosetting polyurethane (TSPU). The polyurethanes (PU) industry is a rapidly expanding business that currently produce some 12 million metric tons of PU raw material annually, with revenues forecast to reach $US 74 billion by the year 2022 [1]. As a result of the wide variety of polyols and isocyanates that are available as raw materials, the structure of the polymer can be modified in order to satisfy specific design requirements for a given application. Subsequently, these polymers have been widely used in applications as diverse as biomaterials for implants [2] as well as in electronic and technological applications [3, 4].

Hollow glass microspheres (HGM) are widely used as fillers of polymer matrix syntactic foams (PSF), as a result of their low heat conductivity and density [5]. PSF are a class of lightweight materials that consist of thin-walled hollow particles, dispersed within a polymer material. These materials are popular due to their ability to provide high specific mechanical characteristics, i.e. specific compressive strength and stiffness, as well as combined with the relative ease of manufacturing associated with such foams. It has been illustrated in several studies that low density polyurethane foams filled with hollow microspheres can enhance the strength and elastic modulus of foams in compression [5–9]. Despite the wide experience accumulated in the field of syntactic foams, it is nevertheless a topical area of study, due to the possibility to tailor the material properties by varying the size, wall thickness and volume-fraction.

In addition to the syntactic foams, one may wish to modify the distribution of the particles in order to enhance the mechanical behaviour of the foams. This may come in the form of a graded structure. The aim of a graded structure is to control the compression deformation behaviour of the material. It has been shown in several studies [10–13] that graded structures can outperform their monolithic counterparts. Graded materials have their composition, density or microstructure changed in the through-thickness direction of the structure. Particularly for dynamic applications, these structures are attractive due to the progressive response under dynamic loading.

Furthermore, reinforcements in terms of embedding composite tubes in

foams can be used in order to further enhance the mechanical properties of such composite structures. There have been several studies reported on the axial crushing behaviour of composite and metallic tubes [14–21]. The purpose of crush tubes is to absorb and convert kinetic energy into gross plastic deformations under severe loading condition. Alia et al. [22] reported the findings of low density polymer foams reinforced with T700 CFRP tubes, with promising results. The specific energy absorption (SEA) was shown to increase with decreasing inner diameter to thickness (D/t) ratio and it was shown that a tube with a D/t ratio of 6.3 provided the highest energy absorption per unit mass.

The aim of this research was to combine the aforementioned parameters, i.e. fillers, tubes and functionally graded foams (FGF), into one structure, to optimise the structural response under static and dynamic loading conditions. To date, there has been limited research on such structures. These materials may be suited to a number of energy-absorbing structures, such as those employed in automobiles, aircraft and ships, where crash safety is of great importance. In order to optimise the mechanical properties of syntactic TSPU (casting resin), the volume fraction of HGMs is varied systematically. Furthermore, to control the load during compression in energy absorbing structures, developments in the grading of the syntactic foams are made, resulting in FGF. The work was extended via the introduction of CFRP tubes into the TSPU (syntactic and non-syntactic) to increase in SEA for static and dynamic applications, with comparisons made against CFRP reinforced polyether TPU.

2. Experimental methodology

2.1. Manufacturing

TSPU, a highly cross-linked polymer, was manufactured using vacuum assisted resin transfer moulding (VARTM). The TSPU has two parts, the resin (Part A) - the formulated polyol was mixed with hollow glass microspheres (K20 series, $\phi = 30 - 115\mu m$, $\rho = 0.2g/cc$) [23] for several minutes to ensure that the microspheres were well distributed, after which the hardener (Part B) - the isocyanate - was added to the mixture. The mix ratio of both components was 100:100 gram/gram. The resin was transferred through a channel and into the 200 x 200 mm mould with a depth of 20 mm. However, prior to this a vacuum pump was attached to the outlets, to minimise the

amount of trapped air and enabling the resin to flow into the mould by introducing a pressure difference. Figure 1 shows the density variations of the syntactic TSPU as a function of the percentage of microspheres within the matrix. M0 is defined as the pure TSPU, without any microspheres and M1 - M12 refer to the syntactic TSPU with varying levels of density.

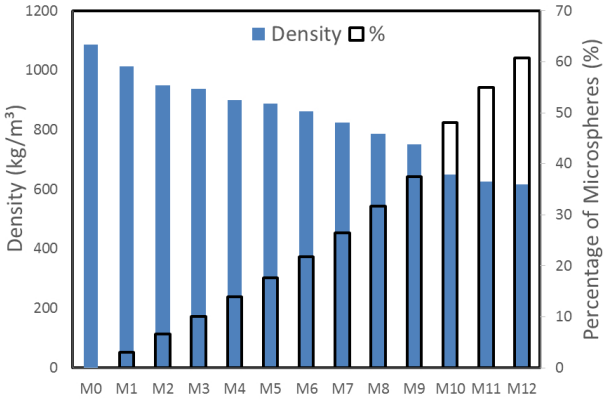

Figure 1: Variation of hollow glass microspheres (%, volume) and density (kg/m^3) of the syntactic TSPU.

The volume fraction of the microspheres is calculated using the following equation,

$$\frac{W_{SF}}{V_{SF}} = \rho_{GM} \cdot (f_{GM}) + \rho_{PU} \cdot (1 - f_{GM}) \tag{1}$$

where W_{SF} and V_{SF} are the measured weight and volume of the syntactic foam. ρ_{GM} and ρ_{PU} represent the densities of the glass microspheres and the resin, respectively. The density of the TSPU resin is approximately 1087 kg/m^3. Rearranging Equation (1) provides the volume fraction of the microspheres (f_{GM}) as

$$f_{GM} = \frac{\rho_{PU} - \rho_{SF}}{\rho_{PU} - \rho_{GM}} \tag{2}$$

where ρ_{SF} represents the density of the syntactic foam.

During the manufacturing process one cannot fully ensure the hollow microspheres are fracture free. Careful processing is advisable but may not completely eradicate this issue. Fracturing of the spheres would open up

their cavity, which could subsequently be filled with the resin. Therefore, the volume fraction of microspheres can only be provided as an approximation.

Figure 2a presents an example (TSPUG1) of one of the graded foams used in this study, with a four-density variation at a 5 mm depth increment. Figure 2b shows an optical micrograph taken on the surface of the composite with a surface finish of approximately $5\mu m$, which illustrates the dispersion of the microspheres within the TSPU matrix. The investigation on the stepwise graded foams i.e. G1 and G2, uses the different densities for the individual foams as detailed in Table 1.

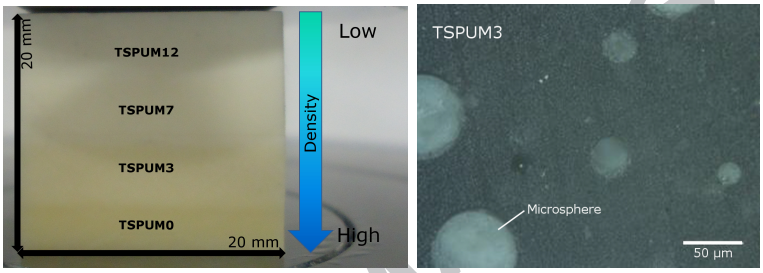

(a) TSPUG1 cross-section (b) Optical micrograph

Figure 2: (a) Example of the cross section of stepwise graded foam (TSPUG1), with density variation through-thickness and (b) optical micrograph of TSPUM3 illustrating the embedding of glass microspheres in the TSPU matrix.

Table 1: Density variation through the thickness of the graded TSPU specimens G1 and G2.

Thickness (mm)	G1	G2
0-5	M0 (1087 kg/m^3)	M0 (1087 kg/m^3)
5-10	M3 (937 kg/m^3)	M3 (937 kg/m^3)
10-15	M7 (825 kg/m^3)	M7 (825 kg/m^3)
15-20	M12 (617 kg/m^3)	

TPU is a linear segmented block copolymer consisting of hard and soft segments that can be moulded when heated before returning to a solid phase when cooled. Specimens based on the polyether grade TPU (Desmopan DP 9852 [24]) were used in this study and manufactured using a hot press. The TPU pellets were pre-dried at 110 $°C$ for 3 hours and placed into a mould that was initially heated to $50°C$. In order to prevent the sample from sticking to

the mould, a silicon based grease was applied on the interior surface of the 150 mm by 150 mm mould. A pressure of 350 kPa and a temperature of 220 $^{\circ}C$ were maintained for 25 minutes. The specimen was then cooled at room temperature and removed from the mould when the temperature was below 50 $^{\circ}C$. The specimens were then washed with distilled water, followed by washing with ethanol in order to minimise contamination. The TPU panels had a density of 1150 kg/m^3. For the reinforcement, T700 unidirectional carbon fibre tubes, with a density of 1600 kg/m^3 and an outer diameter of 10 mm (D/t ratio = 6.3), were embedded within the TSPU and TPU matrix. The arrangement of the tubes in the TSPU and TPU is illustrated in Figure 3.

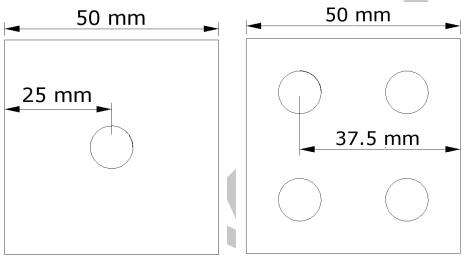

(a) One tube. (b) Four tube.

Figure 3: One and four CFRP tube configurations used with the TPU and TSPU matrices.

2.2. Mechanical testing

Compression tests on the TPU and TSPU specimens were carried out on a 100 kN Instron *4505* universal servo hydraulic testing machine. Tests were performed with loading axis orientated in the "through the thickness" direction. A 600 kN Instron *5989* was used to test the reinforced specimens. Standard laboratory conditions were 23 ± 2 $^{\circ}C$ with 30-40% relative humidity. For the quasi-static compression testing, the sample dimensions were 20 x 20 x 20 mm. In order to minimise friction between the platen and the specimens, both platens were greased. The cross-head displacement rate was set to 1 mm/min and at least three repeated tests were conducted for each material. The specific energy absorption, E_s, is defined as:

$$E_s = \frac{(\int_0^{\epsilon_d} \sigma \cdot d\epsilon)}{\rho} \tag{3}$$

where ϵ_d is the densification strain and ρ is the density of the sample.

Instrumented drop-hammer tests were also undertaken to investigate the influence of a higher strain rate on the mechanical properties of the specimens. A drop mass of 25.6 kg was used for the lower energies (64 - 276 J) for the samples without tube reinforcements. The variation of load with time was measured with the use of a Kistler piezo-electric load cell (maximum capacity = 120 kN), located between the carriage and the flat impactor, as shown in Figure 4a. Loading data was acquired as voltage output and transferred into a module 64K Data Acquisition Station (DAS) at a frequency of 100 kHz. A High Speed Camera (HSC) was used to measure displacement and velocity. For the reinforced samples, an impact rig set up with a drop weight mass of 107.5 kg was used, as shown in Figure 4b, which provided higher impact energies (360 - 2046 J). The variation of velocity and time was measured using a Dantec Flowlite laser Doppler velocimeter (LDV) system [25], to obtain load and displacement data. The LDV system used in this study includes a Burst Spectrum Analyser (BSA) enhanced signal processor model 57N21, which was linked to a computer via an interface card, optic unit and a fibre optic cable.

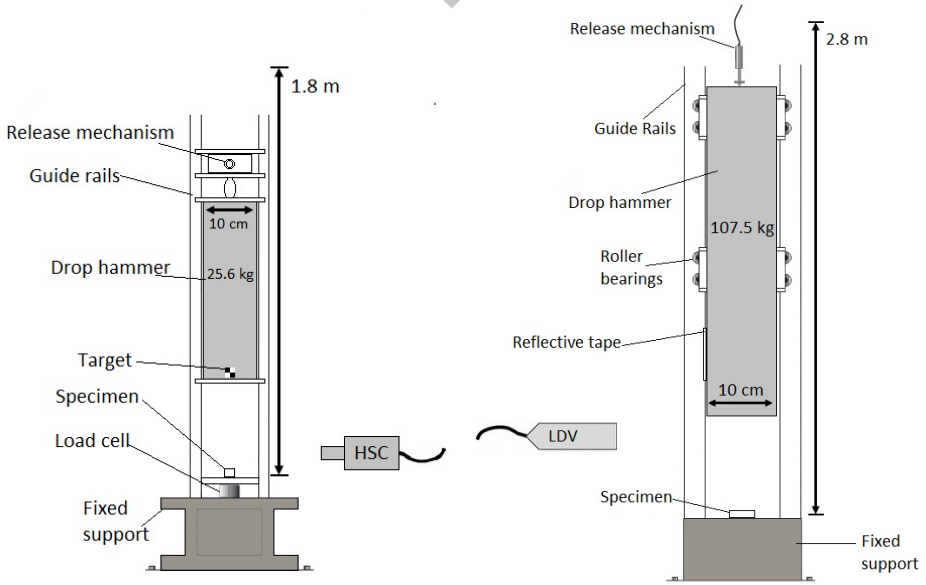

(a) HSC (b) LDV

Figure 4: HSC impact rig set up for unreinforced samples (4a) and LDV impact rig set up for tube reinforced samples (4b).

3. Results and Discussion

3.1. Quasi-static compression test results

3.1.1. Unreinforced syntactic TSPU

The energy absorption of the specimens loaded in quasi-static compression was calculated up to the onset of densification. Figure 5 presents the energy absorbed and energy absorbed per unit mass (SEA) for the TSPU samples with densities ranging from 617 to 1087 kg/m^3. Evidence presented in Figure 5 shows that SEA can be increased slightly throughout the various densities. The highest value was observed at 937 kg/m^3, for the syntactic foam M3.

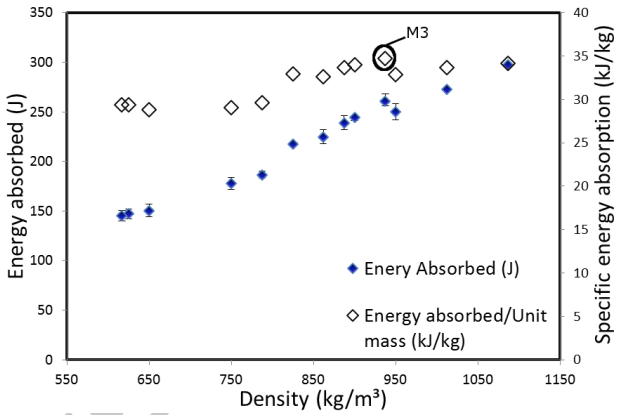

Figure 5: Energy absorbed and specific energy absorbed for TSPU (M0-M12).

Figure 6 shows typical stress-strain curves following the compression tests on the TSPU foams (M0, M3, M7 and M12), where it is evident that the plateau regions are extended slightly due to the collapsing of the microspheres inside the syntactic TSPU. The empty cells which are introduced by the hollow microspheres reduce the strength of the syntactic foam by weakening the matrix via the introduction of stress concentrations.

The deformation mechanisms are presented in Figure 7 for the non-syntactic TSPU M0, syntactic M12 and graded G1, where it can be seen that M0 exhibits a more ductile failure, whereas M12, which is dominated by shear bands, experiences a more brittle failure. The graded foam attempts to combine the characteristics of the individual foams, via incrementally-graded thickness profile. G1 demonstrates a more progressive failure mode which can be a benefit under dynamic loading, whereby the foremost layer

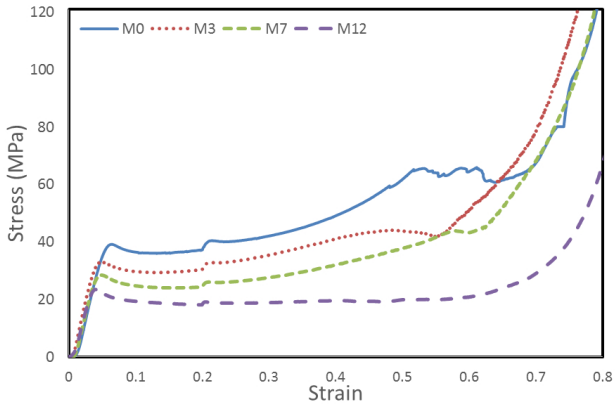

Figure 6: Stress-strain curves for TSPUM0, M3, M7 and M12 under quasi-static loading.

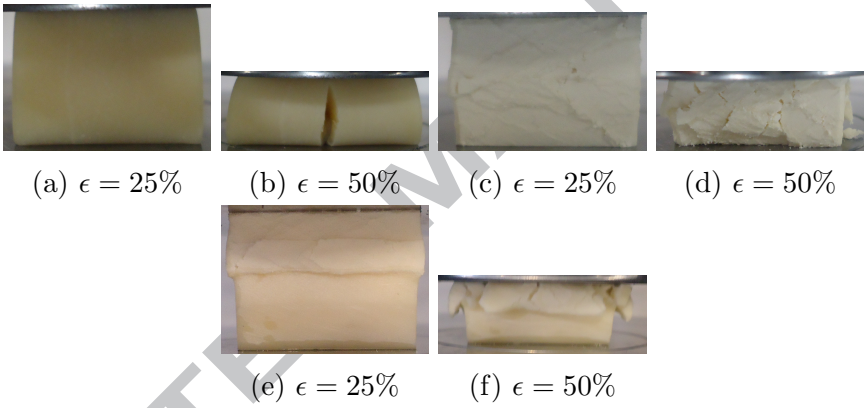

(a) $\epsilon = 25\%$ (b) $\epsilon = 50\%$ (c) $\epsilon = 25\%$ (d) $\epsilon = 50\%$

(e) $\epsilon = 25\%$ (f) $\epsilon = 50\%$

Figure 7: Photographs of the collapse mechanisms of M0 (7a, 7b), M12 (7c, 7d) and G1 (7e, 7f) under quasi-static loading.

offer both high energy absorption characteristics and dampening properties, whereas the rearmost layer offers a higher compressive stiffness.

3.1.2. CFRP tube reinforced TSPU and TPU

With the introduction of CFRP tube reinforcements, one can observe that the stress-strain curves, displayed in Figure 8, clearly exhibit a significant improvement in the compressive strength of both TSPU and the TPU systems. For example, the stress-strain plot for the unreinforced TPU did not clearly indicate a yield point, the addition of tubes help in improving the stiffness of the TPU under quasi-static loading conditions by providing a higher peak stress.

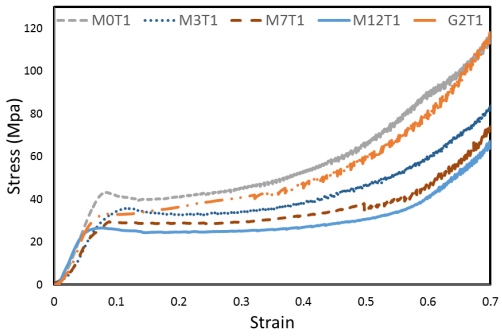

(a) One tube reinforced TSPU

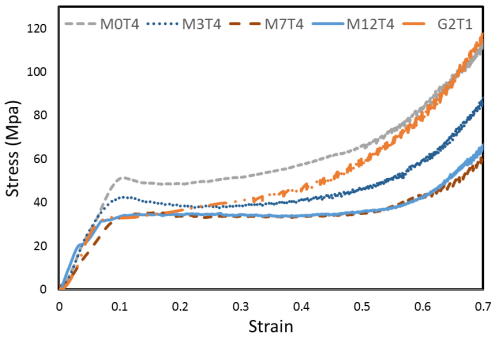

(b) Four tube reinforced TSPU

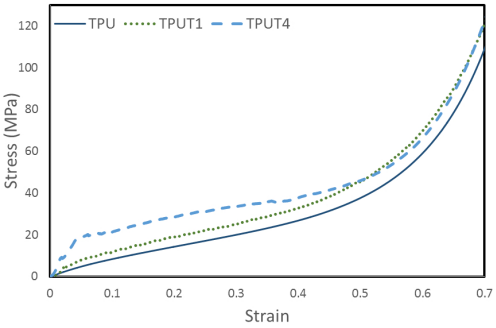

(c) Unreinforced and reinforced (One and four tubes) TPU

Figure 8: Quasi-static stress vs. strain curves for (8a) 1 CFRP tube reinforced TSPUM0, M3, M7 and M12, (8b) 4 CFRP tube reinforced TSPUM0, M3, M7 and M12 and (8c) unreinforced and reinforced 1 and 4 tube TPU.

Figure 9 presents the SEA and plateau stresses at 25 % and 50 % for the unreinforced and reinforced syntactic TSPU foams under quasi-static loading conditions. The addition of CFRP tubes can significantly improve the energy absorbing characteristics of the TSPU and TPU under quasi-static loading conditions. The addition of a single tube (T1) increases the SEA of M0 by 21.5 %. The highest increase can be seen with M12T4 (T4 = four tubes), which has a SEA of 56.28 kJ/kg, providing an increase of 47.7 % relative to the unreinforced foam, M12. The plateau stress is an important consideration in the design of crash protective structures. The structure must absorb the kinetic energy of a moving object without reaching its densification strain, whilst ensuring that the transmitted stress never exceeds the plateau stress. It can be seen that in addition to enhancing

the SEA, in all cases the reinforcements increase the plateau stress for all densities.

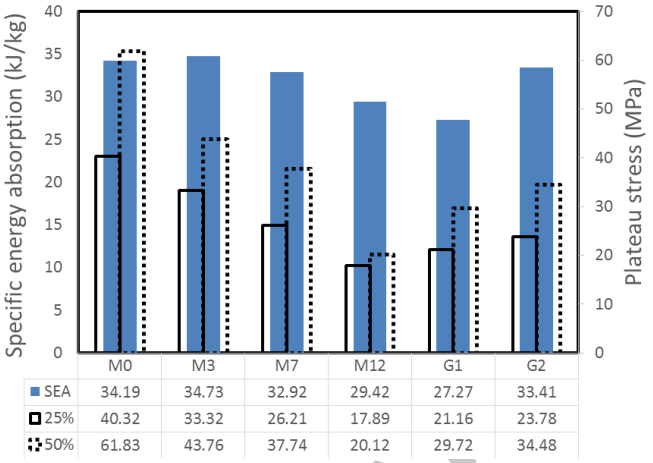

	M0	M3	M7	M12	G1	G2
SEA	34.19	34.73	32.92	29.42	27.27	33.41
25%	40.32	33.32	26.21	17.89	21.16	23.78
50%	61.83	43.76	37.74	20.12	29.72	34.48

(a) Unreinforced

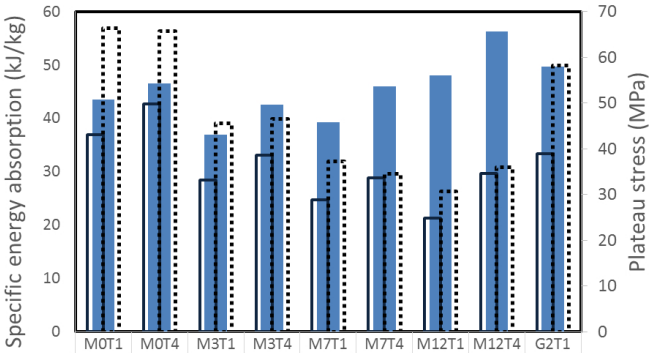

	M0T1	M0T4	M3T1	M3T4	M7T1	M7T4	M12T1	M12T4	G2T1
SEA	43.55	46.49	36.88	42.59	39.25	45.93	48.09	56.28	49.66
25%	43.03	49.81	33.23	38.55	28.92	33.64	24.84	34.61	38.92
50%	66.34	65.67	45.65	46.56	37.26	34.54	30.69	35.91	58.26

(b) Reinforced

Figure 9: SEA and plateau stresses at 25% and 50% for the unreinforced (9a) and reinforced (9b) syntactic TSPU under quasi-static loading.

In order to compare the specific performance of the syntactic foam under quasi-static loading conditions, a comparison of the syntactic foam has been made with a wide variety of materials, as shown in Figure 10. This plot considers the specific compressive strength (σ_c/ρ) and specific compressive stiffness (E/ρ) as an indication of performance of the unreinforced and CFRP tube reinforced syntactic TSPU. M12, which has the lowest density,

provides a much higher specific compressive stiffness than M0, with a percentage increase of 95 %, whilst the compressive strength is shown to have an increase by just 8.6 % on average. Nevertheless, the best performing reinforced foam, M12T4, is shown to provide a substantial increase (i.e. 65 %), in specific compressive strength with an average value of approximately 55 $kPa/(kg/m^3)$. The specific compressive strength is also shown to be relatively competitive in relation to the honeycombs and metals. It should be noted that the composition and the density of the syntactic TSPU have a dominant effect on the specific mechanical properties of the CFRP reinforced foams.

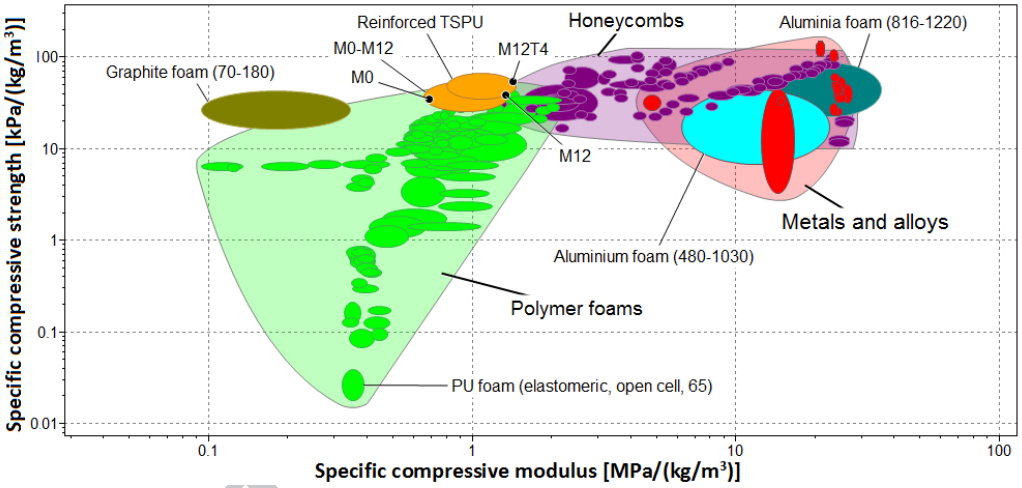

Figure 10: Ashby plot comparing the specific compressive properties of the unreinforced/reinforced non-syntactic TSPU M0 and syntactic TSPU. Material data from Ref. [26].

3.2. Dynamic compression test results

3.2.1. Unreinforced syntactic TSPU and TPU

Before considering applications of syntactic TSPU and TPU as energy absorbers, it is necessary to investigate their dynamic behaviour. Ideally, a prolonged constant plateau stress level is required to provide the maximum area under the stress-strain curve. There are various parameters that are associated with rate-sensitivity in cellular materials, i.e. solid material rate-sensitivity, pressure of the trapped air in the cells and micro-inertia effects. The impact response, as depicted in Figure 11 for the ungraded TSPU, is

shown to be inconsistent with the response observed under quasi-static loading, illustrating the materials sensitivity to an increase in strain rate. The ungraded foams are characterised by the initial peak stress, although higher than the static tests, it is then followed by a significant drop in stress with some oscillations in the stress-strain trace. A reduction of this order can be described as complete failure in a large number of applications, indicating shattering fracture of the specimen.

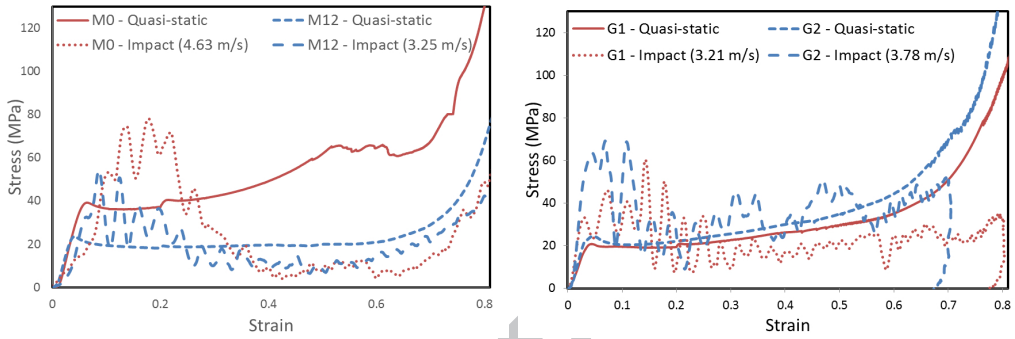

(a) M0 and M12 (b) G1 and G2

Figure 11: Quasi-static vs. dynamic stress-strain curves for (11a) M0 and M12, (11b) G1 and G2.

The oscillatory behaviour is most likely due to the dynamic effects in the load cell and drop-weight carriage, in addition to the instabilities in the fracture process. Subsequently, the dynamic behaviour of both of the graded foams show a plateau region with a nearly constant stress. G1, which is based on a greater variation in densities, provides a more prolonged plateau region than G2, which is consistent with the results of the quasi-static tests. However, G2 exhibits higher plateau stresses, showing an increase of 83.6 % in stress at 50 % strain. Furthermore, the stiffness of both M0 and M12 were shown to be lower under dynamic loading than quasi-static conditions. However, the peak stresses show a significant increases, highlighting the strain-rate sensitivity of the TSPU material. On the other hand, the graded foams (G1 and G2) provide a slightly higher stiffness under dynamic loading than quasi-static loading, in addition to increased peak stresses. Figure 12 shows that the plateau stresses for M0 under impact are much lower than that of the quasi-static tests. A similar response was observed for M12 under impact. The plateau stresses for the graded foams however, indicate a significant improvement in comparison to the ungraded foams.

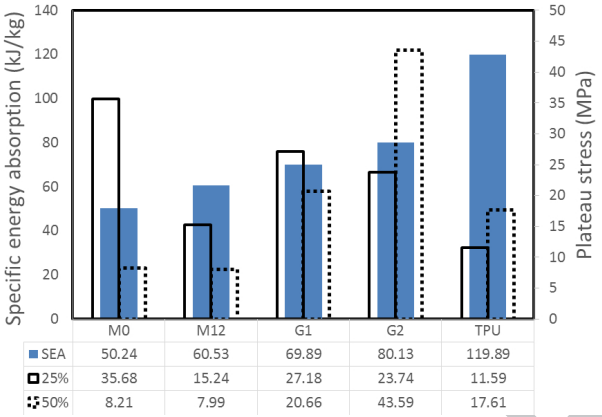

Figure 12: SEA and plateau stresses at 25% and 50% for the unreinforced TSPU and TPU under dynamic loading

Low velocity impact tests were also carried out on the TPU specimens, with the results presented in Figure 13. Here, five impact velocities were tested. Figure 13a shows three of those at strain rates of 117, 174 and 207 s^{-1}. These experiments illustrate the strong rate dependence and features of the stress-strain behaviour of TPU. Under impact, composite materials experience large amounts of strain which is dependent upon the magnitude of the impact, temperature range and strain rates. The nature of the stress-strain curve clearly shows the rate dependency of the TPU. The ratio of the dynamic to static initial peak stresses and plateau stress notably increase with increased impact energy, and present the TPU with increased SEA characteristics, as shown in Figure 13b. Furthermore, the underlying material structure of the TPU is also shown to undergo significant changes with the increased impact energy, with significant deformations being observed from 735 to 1155 J (174 - 207 s^{-1}). Within the polyurethane family, TPU is popular, due to its ability to alter its microstructure and thus its mechanical behaviour. In many TPUs, the hard domains are immersed in a soft (rubbery) segment matrix [27]. Since hard domains occupy a significant volume and are stiffer than the soft domains, they function as an effective nanoscale filler and provide similar material behaviour to that of a composite. The ability of TPUs in altering its microstructure and therefore its mechanical behaviour [28], presents TPU as an attractive polymeric material for such applications.

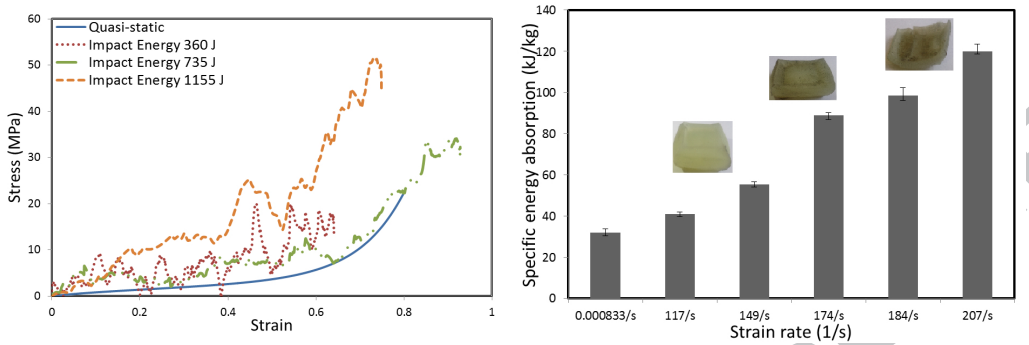

(a) Stress vs. strain (b) Specific energy absorbed

Figure 13: Stress vs. strain (13a) and SEA vs. strain rates (13b) for TPU under dynamic loading.

3.2.2. CFRP tube reinforced TSPU and TPU

Figure 14a shows the TPU and syntactic TSPU impact responses, with one tube reinforcement. As was the case for the unreinforced TSPU, the behaviour of the reinforced TSPU is characterised by an initial peak followed by a significant drop in the stress. The reinforced TPU under dynamic loading is much stiffer, in distinct contrast to the TPU without reinforcement under quasi-static loading. Furthermore, the reinforced TPU shows a progressive response with the stress increasing in three steps, making it ideal for dynamic applications by providing a steadily increasing energy absorption capacity.

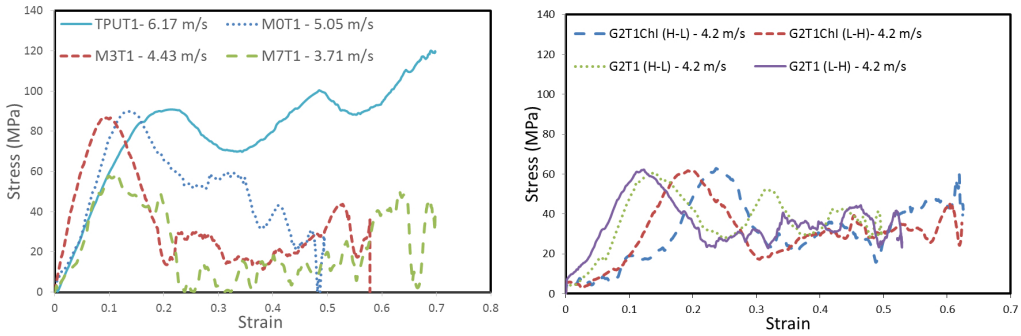

(a) Reinforced M0, M3, M7 and TPU (b) Reinforced G2

Figure 14: Stress vs. strain traces for (14a) reinforced TPUT1, TSPUM0T1, M3T1, M7T1 and (14b) reinforced G2 with and without chamfered tubes.

Furthermore, a direct comparison was made in relation to tubes with and

without a chamfer (ChI) embedded in the graded TSPU specimen, G2. In addition to testing the samples with a low-high density (L-H) and high-low density (H-L) grading. The dynamic stress-strain traces are shown in Figure 14b. A single chamfer 45° on the inner diameter of the tubes were used. Introducing a chamfer to one end of a CFRP tube can initiate crushing, where failure begins at the chamfer tip and the damage zone propagates in the axial direction of the tube without catastrophic failure. It is shown that the initial peak stress in chamfered tubes is delayed relative to unchamfered tubes. This is consistent with both H-L and L-H layups, with H-L providing a slightly more delayed peak stress response.

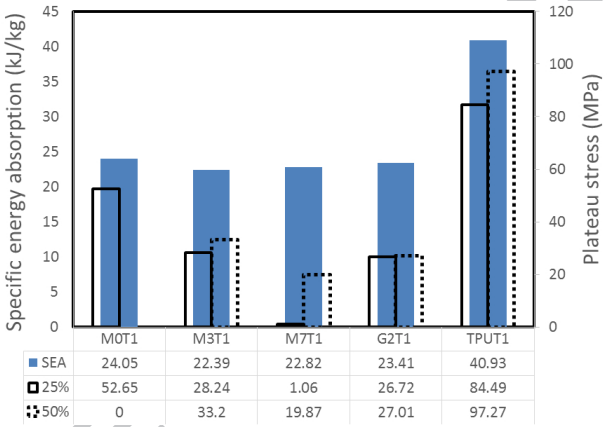

	M0T1	M3T1	M7T1	G2T1	TPUT1
SEA	24.05	22.39	22.82	23.41	40.93
25%	52.65	28.24	1.06	26.72	84.49
50%	0	33.2	19.87	27.01	97.27

Figure 15: SEA and plateau stresses at 25 % and 50 % strain for the reinforced foams under dynamic loading.

The plateau stresses for the reinforced TSPU and TPU under dynamic loading are presented by Figure 15. In comparison to the unreinforced TPU (Figure 13a), the reinforced TPU yielded 629 % and 452 % increases in plateau stresses at 25 % and 50 % strain, respectively. The potential of the reinforced TPU under dynamic loading is further illustrated by the SEA values, with TPUT1 providing the highest SEA. Although the specific energy absorption is lower than that of the unreinforced 20 x 20 x 20 mm TPU samples, due to the limitations of the drop weight tower it is expected that the SEA values for the tube reinforced TPU could increase proportionally for higher impact energies, where more significant deformations of the reinforced TPU may be observed. Figure 16 illustrates the brittle nature of the TSPU sample and the enhanced integrity of the TPU under impact, where it can be seen that the latter retains most of its original shape, whilst the tubes in

both cases fragment into small debris.

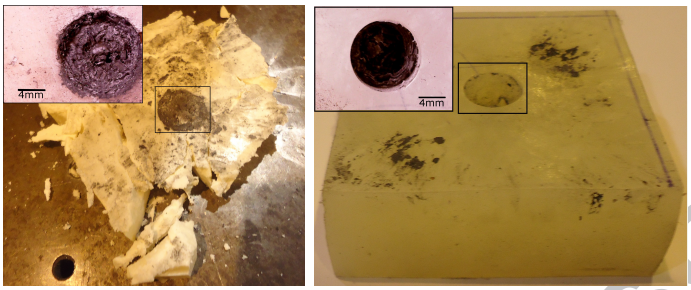

(a) M0 (b) TPU

Figure 16: Typical failure of reinforced (16a) TSPUM0 and (16b) TPU samples under dynamic compressive loading.

4. Conclusions

Investigations of syntactic TSPU and TPU with and without the embedded CFRP tubes under both quasi-static and dynamic loading have been carried out. The load bearing capacity of the CFRP tube reinforced syntactic TSPU foams was increased significantly relative to the unreinforced syntactic TSPU, where SEA increases as high as 48 % (56.28 kJ/kg) were noted. In addition, specific compressive strength (σ_c/ρ) increased by 65 % reaching 55 $kPa/(kg/m^3)$. However, the post-yield behaviour under dynamic loading was reduced. The pure TSPU (no glass microspheres), for example, experienced stain-hardening under quasi-static loading, whereas under dynamic loading it exhibited a significant drop in the plateau stress. This behaviour was consistent with the syntactic foams (with glass microspheres). Improvements in the plateau levels were made by introducing a graded structure, since it resulted in a more progressive response and a relatively constant stress level under dynamic loading. Future work on the syntactic foams, could include modifications of the size, wall thickness and/or type of microspheres. Further optimisation in the specific mechanical characteristics and improvements in the impact response can be made with further variations in distribution of the microspheres.

Furthermore, the specific energy absorption characteristics of TPU under dynamic loading was shown to increase with increasing impact energy, making them an attractive prospect to structural impact applications. The

incorporation of CFRP tubes into the TPU greatly improved their properties and presents the reinforced TPU with greater energy absorbing characteristics under dynamic loading conditions.

Acknowledgements

The authors would like to thank the University of Manchester for allowing us to use their testing facilities (600 kN Instron *5989*). The authors also greatly appreciate Covestro for providing the Desmopan DP 9852 TPU pellets.

References

[1] Ceresana. Market Intelligence. Consulting, `www.ceresana.com`.

[2] V. M. R. Barros, A. L. Rosa, M. M. Beloti, G. Chierice, In *vivo* biocompatibility of three different chemical compositions of *Ricinus communis* polyurethane, Journal of Biomedical Materials Research 67 (2003) 235–239.

[3] G. Wegner, M. Brandt, L. Duda, J. Hofmann, B. Klesczewski, D. Koch, R. J. Kumpf, H. Orzesek, H. G. Pirkl, C. Six, C. Steinlein, M. Weisbeck, Trends in industrial catalysis in the polyurethane industry., Journal of Oleo Science 221 (2001) 303–335.

[4] W. K. Sakamoto, S. Shibatta-Kagesawa, D. H. F. Kanda, S. H. Fernandes, E. Longo, G. O. Chierice, Piezoelectric effect in composite polyurethane ferroelectric ceramics, physica status solidi (a) 172 (1999) 265–271.

[5] V. Yakushin, L. Bel'kova, I. Sevastyanova, Properties of rigid polyurethane foams filled with glass microspheres, Mechanics of Composite Materials 48 (5) (2012) 579–586.

[6] E. Barber, J. Nelson, W. Beck, Improving properties in rigid urethane foams using glass bubbles, Journal of Celluar Plastics 13 (1977) 383–387.

[7] J. A. Hagarman, J. P. Cunnion, B. W. Sands, Formulation and physical properties of polyurethane foam incorporating hollow microspheres, Journal of Celluar Plastics 21 (1985) 406–408.

[8] I. V. Masik, N. V. Sirotinkin, S. V. Yatsenko, S. V. Vakulenko, Effect of glass microspheres on the properties of rigid polyurethane foams, Plasticheskie Massy 30 (3) (2002) 41–46.

[9] X.-C. Bian, J.-H. Tang, Z.-M. Li, Flame retardancy of hollow glass microsphere/rigid polyurethane foams in the presence of expandable graphite, Journal of Applied Polymer Science 109 (3) (2008) 1935–1943.

[10] M. S. Attia, S. A. Meguid, H. Nouraei, Nonlinear finite element analysis of the crush behaviour of functionally graded foam-filled columns, Finite elements in Analysis and Design. 61 (2011) 50–59.

[11] J. Zhou, Z. Guan, W. J. Cantwell, The impact response of graded foam sandwich structures, Composite Structures 97 (2013) 370–377.

[12] Y. Hangai, N. Kubota, T. Utsunomiya, H. Kawahima, O. Kuwazuru, N. Yoshikawa, Drop weight impact behaviour of functionally graded aluminium foam consisting of A1050 and A6061 aluminium alloys, Materials Science and Engineering A 639 (2015) 597–603.

[13] C. Y. Huang, Y. L. Chen, Design and impact resistant analysis of functionally graded $Al_2 - Zr0_2$ ceramic composite, Materials and Design 91 (2016) 294–305.

[14] G. I. Farley, Effect of specimen geometry on the energy absorption capability of composite materials, Composite materials 20 (1986) 390–400.

[15] D. W. Schmusser, I. E. Wickliffe, Impact energy absorption of continuous fibre composite tubes, Engineering Materials and Technology 109 (1987) 72–77.

[16] D. Hull, Unified approach to progressive crushing of fibre reinforced composite tubes, Composite Science and Technology 40 (1991) 377–421.

[17] S. Ochelski, P. Kiczko, A. Static, Axial crush performance of unfilled and foam-filled composite tubes, Bulletin of the Polish Academy of Sciences: Technical Sciences 60 (2012) 31–35.

[18] F. Schneider, N. Jones, Impact of thin-walled high-strength steel structural sections., Proceedings of the institution of Mechanical Engineers, Part D. 218 (2) (2004) 131–158.

[19] A. G. Olabi, E. Morris, M. S. J. Hashmi, Metallic tube type energy absorbers: a synopsis, Thin-Walled Structures 45 (2007) 706–726.

[20] S. C. K. Yuen, G. N. Nurick, The energy-absorbing characteristics of tubular structures with geometric and material modifications: an overview., Applied Mechanics Reviews. 61 (2) (2008) 1–15.

[21] M. A. D. Karagiozova, Dynamic elastic-plastic buckling of structural elements: a review, Applied Mechanics Reviews. 61 (4) (2008) 1–15.

[22] R. A. Alia, W. J. Cantwell, G. S. Langdon, S. C. K. Yuen, G. N. Nurick, The energy-absorbing characteristics of composite tube-reinforced foam structures, Composites: Part B 61 (2014) 127–135.

[23] Easy Composites Ltd, `www.easycomposites.co.uk`.

[24] Covestro LLC, `http://www.tpu.covestro.com`.

[25] R. S. Birch, N. Jones, Measurement of impact loads using a laser Doppler velocimeter., Proceedings of the Institution of Mechanical Engineers 204.

[26] CES EduPack, Cambridge UK: Granta design limited (2012).

[27] J. F. Z. Petrovic, Polyurethane elastomers, Prog. Polym. Sci. 16 (1991) 695–836.

[28] J. Yi, M. C. Boyce, G. F. Lee, E. Balizer, Large deformation rate-dependent stress-strain behaviour of polyurea and polyurethanes, Polymer 47 (1) (2006) 319–329.